Scanning superconducting quantum interference device microscope in a dilution refrigerator

Per G. Björnsson
Geballe Laboratory for Advanced Materials and Department of Applied Physics, McCullough Building, Stanford University, Stanford, California 94305-4045

Brian W. Gardner
Geballe Laboratory for Advanced Materials and Department of Physics, McCullough Building, Stanford University, Stanford, California 94305-4045

John R. Kirtley
IBM T.J. Watson Research Center, Yorktown Heights, New York 10598

Kathryn A. Moler[a)]
Geballe Laboratory for Advanced Materials and Department of Applied Physics, McCullough Building, Stanford University, Stanford, California 94305-4045

(Received 30 March 2001; accepted for publication 1 August 2001)

We report on a scanning superconducting quantum interference device microscope operating at temperatures down to 20 mK in a dilution refrigerator. The instrument is designed for studying quantum mechanical coherence effects in mesoscopic systems and investigating magnetic effects on a mesoscopic length scale in novel materials. We have demonstrated the low-temperature operating capabilities of the instrument by studying superconducting tin disks and the superconducting transition of a thin-film tungsten sample and vortices in the same film. Looking forward, we discuss the applicability of the instrument to measurements of persistent currents in normal-metal rings. [DOI: 10.1063/1.1406931]

I. INTRODUCTION

Magnetic probes are of great interest for studying quantum coherence effects such as persistent currents in mesoscopic metallic structures.[1] These mesoscopic effects are generally seen at low temperatures, typically far below 1 K. In order to reach this measurement regime we have built a scanning superconducting quantum interference device (SQUID) microscope in a dilution refrigerator. In addition to studying mesoscopic structures, we anticipate using the system to study magnetic effects on mesoscopic length scales in novel materials.

SQUIDs are useful as magnetic probes of mesoscopic systems since they have the highest flux sensitivity of any available magnetic sensor. A SQUID measures the magnetic flux threading the SQUID loop, and thus provides a direct and quantitative measurement of magnetic effects. Scanning SQUID microscopes have been reviewed by Kirtley and Wickswo.[2] One design for a microscope in a dilution refrigerator has been reported.[3] We demonstrate a simple and functional piezoelectric SQUID microscope, easily adaptable for use in most dilution refrigerators.

Our micro-SQUIDs can function both as magnetometers (measuring the local magnetic field) and susceptometers (measuring the local magnetic susceptibility). Micro-SQUID susceptometers[4,5] have been used in a stationary configuration for studying samples fabricated or placed in one of the pickup loops[5–8] and have recently been adapted for scanning.[9]

Performing susceptibility measurements using a scanning SQUID microscope has several major advantages over fabricating or placing the sample directly in the pickup loops of a stationary SQUID. First, scanning allows measurement of the properties of several mesoscopic samples in a single cooldown, significantly improving the statistics of the measurement. Second, there is more flexibility in the preparation of the sample, since the substrate used for the samples does not have to be the same as for the SQUID. Finally, it is easy to measure the SQUID background signal by simply backing the SQUID away from the sample; with the sample in the SQUID pickup loop, background measurements must be done in a separate cooldown since the sample cannot be removed *in situ*.

II. INSTRUMENTATION

A. The scan head

The scanner is designed to provide a large scan range at low temperatures, while still being compact and providing precise control over the positioning. These objectives are achieved by using an ''S-bender'' scanner, as reported by Siegel *et al.*[10] The scanner is built from two pairs of piezoelectric bimorphs, each with segmented electrodes. One pair of bimorphs connects the base of the scanner to the secondary scan stage, moving it in the *y* direction. The second pair connects the secondary and primary scan stages, providing movement in the *x* direction. A separate bimorph is used for

[a)]Electronic mail: kmoler@stanford.edu

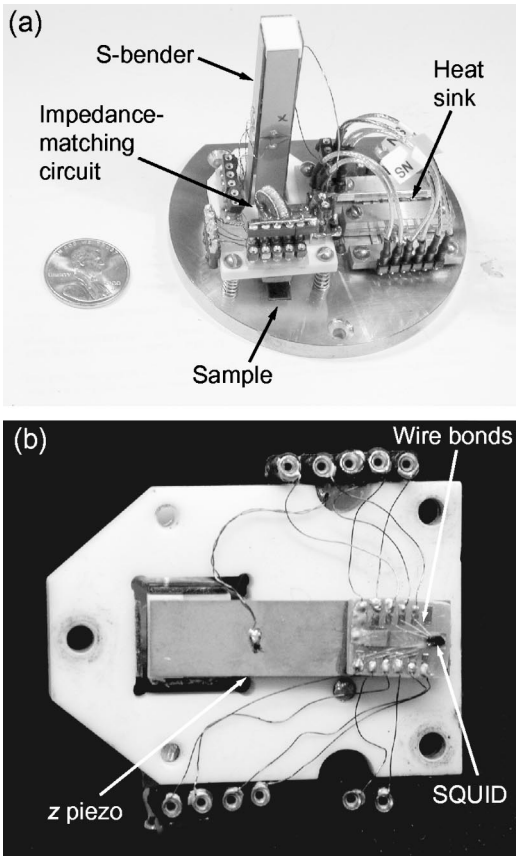

FIG. 1. (a) Photo of the scanner mounted on the copper baseplate. The baseplate is mounted directly to the mixing chamber of the dilution refrigerator. The *z* piezo, attached to the bottom of the S-bender, cannot be seen. (b) The scanner seen from below, with the SQUID mounted on the *z* piezo.

z axis movement. A photograph of the scanner is shown in Fig. 1, and a functional illustration is shown in Fig. 2.

The scanner body elements are machined from MACOR, a machinable ceramic manufactured by Corning Inc., which approximately matches the thermal contraction of the piezo elements. The scanner is mounted with three spring-loaded screws on a baseplate of oxygen-free high-conductivity copper, which is bolted directly onto the outside of the bottom of the mixing chamber of the dilution refrigerator to maximize the thermal contact between the mixing chamber and the sample. The sample is mounted directly on the copper baseplate using silver paint as an adhesive. The three screws used for the scanner mounting allow adjustment of the height and the angle of the SQUID with respect to the sample.

The design intrinsically compensates for thermal contraction of the piezos since the *x* and *y* bimorph pairs are nominally identical.[10] Thus any thermal movement of the scanner will be caused by the MACOR plates and the three mounting screws. The total contraction is estimated to be about 25 μm and is consistent enough between cooldowns that the touchdown point consistently ends up well within the piezo adjustment range of about 15 μm at low temperatures after suitable room temperature adjustment of the touchdown point. This eliminates the need for any low-temperature coarse approach method, vastly simplifying the design.

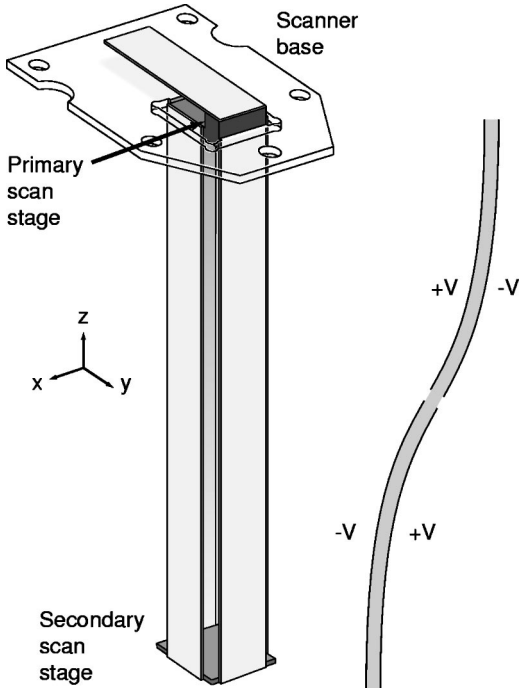

FIG. 2. Sketch of the scan head. One pair of bimorphs moves the secondary scan stage relative to the scanner base along the *y* axis, and the second pair moves the primary scan stage relative to the secondary scan stage along the *x* axis. The shorter bimorph attached to the primary scan stage is used for the *z* axis movement. On the right-hand side is a sketch of the ''S'' shape of a bimorph with segmented electrodes. The ''S-bender'' scanner design was originated by Siegel *et al.* (Ref. 10).

B. SQUID microsusceptometers

The magnetic sensors used in the scanning system are SQUID microsusceptometers designed for scanning as described in Ref. 9. The SQUIDs have two counterwound pickup loops surrounded by field coils, allowing us to locally apply a magnetic field to the sample to perform susceptibility measurements. One of the pickup loops is placed close to the tip of the SQUID so that it is close to the sample when scanning, while the other pickup loop is placed far back on the chip and thus far from the sample. If there is no magnetic response from the sample, equal amounts of flux will pass through both counterwound pickup loops and thus there will be no net contribution from the applied field to the flux through the SQUID. There is a center tap between the field coils that is used to correct for differences in mutual inductance between the two field coil and pickup loop pairs.

The SQUIDs are fabricated to our design by HYPRES, a commercial superconducting electronics foundry. The fabrication differs from the ordinary HYPRES process[11] in choice of material for the resistors shunting the Josephson junctions. The material used in the ordinary process is molybdenum, which is superconducting below 900 mK, so for use at lower temperatures PdAu resistors are substituted. Apart from the different shunt resistor material, the SQUID design is practically identical to the one used in Ref. 9.

The SQUIDs were designed for making susceptibility measurements of mesoscopic samples. However, they can also be used for magnetometry measurements; in this case the field coils can simply be ignored. Different sensors, op-

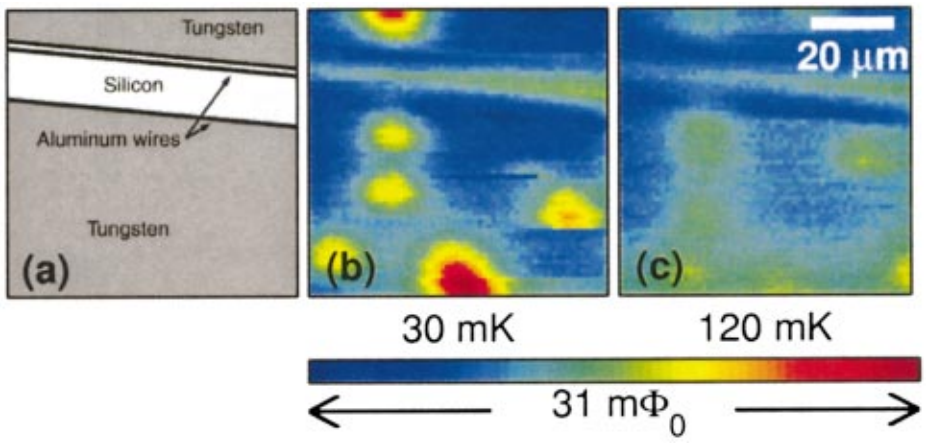

FIG. 3. (Color) (a) Sketch of the W TES sample. (b) and (c) Magnetometry images of vortices at nominal temperatures of 30 and 120 mK, respectively. The images use the same color scale. The small magnitude of the signal indicates that the penetration depth is large compared to the film thickness, and the difference between the images shows that the penetration depth is much larger at 120 mK than at 20 mK.

timized for other measurements, can also be used in the instrument without any major modifications; some examples are dedicated SQUID magnetometers[12] and Hall probes.[13]

C. Shielding and vibration isolation considerations

To reduce stray magnetic fields the refrigerator dewar is surrounded by a three-layer cylindrical μ-metal shield with a triple-layer bottom. The shielding is designed to reduce a lateral field by 81 dB. In order to avoid heating of the sample by radio frequency interference (RFI/EMI) the entire system is enclosed in a rf shielded enclosure. All the signal lines enter the enclosure through a pass-through panel.

The dilution refrigerator is a Kelvinox 100 from Oxford Instruments, designed to minimize the background magnetic field at the sample position by using nonmagnetic materials in the insert and dewar. To minimize vibrational noise, the dewar hangs from a wooden table top which can be floated on optical table legs. Vibrations entering through pumping lines are reduced by using flexible, bellows-style tubing and anchoring all the pumping lines rigidly at the wall of the rf shielded enclosure and passing them through a concrete block. The pumps are in a separate, acoustically isolated room. We have characterized the vibrations at room temperature without floating the table top by using the piezo bimorphs as sensors, connecting an oscilloscope or spectrum analyzer to the electrodes. The rms deviations measured in this way were approximately 0.75 nm in the *x* direction, 7.5 nm in the *y* direction, and 0.125 nm in the *z* direction. Turning on the pumps increased the vibrational noise by less than a factor of 2. These vibrations are not significant for measurements with micron-scale SQUIDs. The lowest resonances of the scanner are at 24 and 30 Hz in *x*, 26 and 30 Hz in *y*, and 22 Hz in *z*.

III. MEASUREMENTS

To test and demonstrate the low-temperature operating capabilities of the instrument, we have studied magnetic effects in tungsten thin films, both in SQUID magnetometry and susceptometry mode, and tin disks previously studied at higher temperatures[9] in susceptometry mode.

A. Vortices in a tungsten thin film

The tungsten thin film sample that we have studied is part of a transition edge sensor (TES), a photon energy sensor used for astrophysics experiments.[14] The resistive T_c of the sample used in our measurements occurred between 146 and 148 mK.

The section of the sample within the scan range had a large area of thin film W at the bottom of the scan area. At the top of the scan area is a set of Al rails, normally used for TES transport measurements. The rails are separated by an area of bare silicon, and the upper rail is actually two Al lines. At the very top of the images there is a small section of a second W region. A sketch of the sample geometry is shown in the leftmost image in Fig. 3.

For these measurements we calculated the height of the pickup loop above the sample by fitting the SQUID response in an applied dc background field to a model for the response of the aluminum rails. The scans were done with the tungsten in the normal state, so the only significant signal came from the Al rails. The height of the SQUID above the sample in this case was calculated to be 2.5–3 μm.

We have studied magnetic vortex behavior in the W thin film sample in the superconducting state using the instrument in magnetometry mode. Figures 3(b) and 3(c) show typical images of vortices at nominal temperatures of 30 and 120 mK. At all of the vortex sites the flux passing through the pickup loop of the SQUID is a small fraction of a flux quantum Φ_0, indicating that the vortices are spread out over an area larger than the pickup loop. This is caused by a large penetration depth, which can in principle be calculated from the peak height of the measured signal.[15] Taking background uncertainties into account, a rough estimate of the signal amplitude is $20\,\mathrm{m}\Phi_0$ at 30 mK [Fig. 3(b)] and $7\,\mathrm{m}\Phi_0$ at 120 mK [Fig. 3(c)]. Fitting these values to the magnetic flux passing through the SQUID pickup loop in the limit of negligibly short coherence length[15] gives an effective penetration depth $\Lambda(\Lambda=\lambda_L^2/d$, where λ_L is the London penetration depth and d is the thickness of the film, here approximately 40 nm) of 1.5 μm at 30 mK and 2.7 μm at 120 mK.[16]

The vortices typically appear in a few particular spots in the images, indicating that there are preferred pinning sites. However, the images can differ in terms of which pinning sites are populated even between images that are taken im-

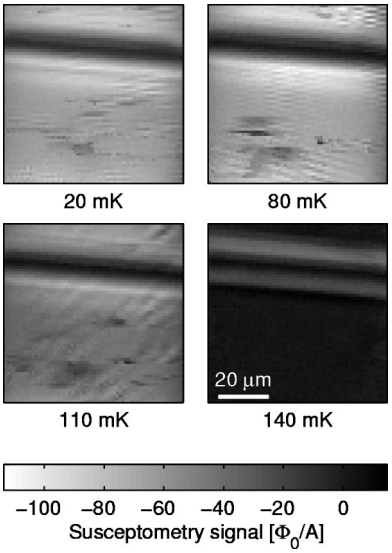

FIG. 4. Susceptibility images of a W TES sensor at different temperatures, covering the same area as Fig. 3. The current through the field coils surrounding the pickup loops is 50 μA rms at 200 Hz. The susceptibility does not change significantly at temperatures below 80 mK; above this temperature the diamagnetic response of the film decreases gradually until the sample is completely in the normal state at 140 mK.

mediately after each other. In some cases we see parts of vortices, indicating that they moved during the scan. An example of this can be seen in the lower right corner of Fig. 3(b). The vortex motion indicates that pinning is actually quite weak in the sample.

B. Superconducting transition in a tungsten thin film

We have performed low-field susceptibility measurements on the W thin film sample in a nominal temperature range between 20 and 150 mK (Fig. 4). The field was applied using a 50 μA rms current through the on-chip field coils, giving a magnetic field of approximately 30 mG rms at the center of the pickup loop when no sample is present.

Up to 80 mK there is no detectable decrease in the magnitude of the susceptibility of the thin films. As the temperature is increased above 100 mK the sample appears quite inhomogeneous. The magnetic response of the sample decreases gradually until the sample is entirely in the normal state at 140 mK. The transition seen in resistive measurements on this sample at 146–148 mK is much sharper than that seen in these susceptibility measurements. The difference in measured T_c and transition width may be caused by the fact that the low-current transport measurements detect the first superconducting path across the sample, while the susceptibility measurements average the signal over an area comparable to the SQUID pickup loop, and thus measure a local average of the T_c.

The thermal contact between the sample and the mixing chamber appears to be sufficient for the sample to reach a given temperature as soon as the mixing chamber temperature has stabilized, at least at temperatures above 100 mK where the temperature dependence of the susceptibility is obvious. This is demonstrated by the similarity of the images

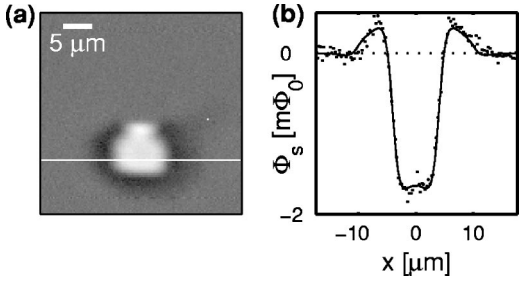

FIG. 5. (a) Susceptibility image of a Sn disk with a diameter of 3 μm. The current through the field coils is 100 μA rms at 200 Hz. The white line indicates the row used for the fit. The full-scale response in terms of flux through the pickup loop relative to the current through the field coils is approximately $20\,\Phi_0$/A. (b) Fit of the susceptibility of the disk using the method described in Ref. 9. The two fit parameters are the dipole moment of the disk and the height of the pickup loop over the sample.

taken while ramping the temperature up and down, no hysteresis is noticeable to within less than 10 mK.

C. Susceptibility of tin microdisks

We have demonstrated the functionality of the scanner in a dilution refrigerator environment by studying the magnetic susceptibility of 3 μm Sn disks with 30 μm spacing at temperatures down to 30 mK. This same sample had previously been used for similar studies in another scanning SQUID susceptometer with a temperature range down to 1.5 K.[9] The results from the measurements performed in the dilution refrigerator setup were, as expected, very similar to the results well below the superconducting transition in the other system.

Because of the well-known geometry of the array of Sn disks we can calibrate the scan range using the array images. The scanner movement is approximately 0.2 μm/V at the lowest temperatures giving a total scan range of about 80 μm. This scan range is limited by our high-voltage amplifiers, which have a maximum output of ± 100 V.

By fitting the scan data to the calculated SQUID response we can calculate the height of the pickup loop above the sample and the dipole moment of the Sn disks.[9] The height was determined to be 1.9 μm, and for the disk shown in Fig. 5 the susceptibility obtained from the fit was $-5 \times 10^7 \mu_B$/G. This susceptibility is consistent with the susceptibilities measured on disks on the same sample in previous experiments at around 2 K.

IV. FIGURES OF MERIT

A. Current performance

The scanner has a scan range of $80 \times 80\,\mu\text{m}^2$ at dilution refrigerator temperatures. We have not observed any temperature dependence of the scan range throughout the dilution refrigerator operating temperature range.

The base temperature of the dilution refrigerator without any energy-dissipating devices connected to the mixing chamber was measured to be less than 11 mK using nuclear orientation thermometry. Although rapid scanning would add a significant heat load to the mixing chamber, the effect of a static voltage on the piezos should be small. Our practical

experience is that the base temperature for measurements is around 15 mK; this may be improved by better thermal management of the wiring.

The SQUID and associated electronics have a white noise background of less than $50\,\mu\Phi_0/\sqrt{\text{Hz}}$ up to the bandwidth limit of the SQUID controller, approximately 400 Hz. This noise level is limited by the performance of the electronics.

The height of the pickup loop above the sample is important both for the spin sensitivity and for the spatial resolution of the instrument. It is determined by the angle between the SQUID and the sample, and by the distance from the pickup loop to the tip of the SQUID. With our current SQUIDs the angle is limited to about 2.5° by the wirebonds to the SQUID, and we typically polish the SQUID so that the center of the pickup loop is 30 μm from the tip. The pickup loop is also covered by a 0.5 μm layer of SiO_2. Altogether this currently limits the proximity of the pickup loop to the sample to slightly less than 2 μm.

We can define the spin sensitivity as the sensitivity to a dipole centered in the pickup loop with the direction of the dipole moment perpendicular to the plane of the SQUID. With a SQUID flux sensitivity of $50\,\mu\Phi_0/\sqrt{\text{Hz}}$ and the current pickup loops, the spin sensitivity is $10^5\,\mu_B/\sqrt{\text{Hz}}$.

B. Possibilities for improvements

The scan range could be improved by using higher voltages to drive the piezos to attain a scan range which is about twice as large. For an even larger range, longer piezos can be used, which would increase the vibrational noise and lower the resonant frequencies of the scanner. However, the current vibration level appears to be far below what would be significant for micron-scale SQUIDs so a small increase in the vibration level may not cause any loss of sensitivity.

The flux sensitivity could be improved with new electronics to reach the intrinsic noise level of the SQUID and with improved SQUID designs. First, SQUIDs have been reported with an intrinsic flux noise level well below $1\,\mu\Phi_0/\sqrt{\text{Hz}}$.[17] Second, using smaller pickup loops and field coils would improve both the spatial resolution and the spin sensitivity. It would also allow us to polish or etch the point of the SQUID closer to the pickup loop, reducing the minimum height of the pickup loop above the sample. Further reductions of the height can be accomplished by not having the pickup loops covered by an SiO_2 layer and by repositioning the wirebond pads on the SQUID, reducing the minimum angle between the SQUID and the sample. A height of 0.5 μm above the sample should be attainable.

The spin sensitivity can be improved both by improved flux sensitivity and by improved coupling between the dipole and the SQUID. Improving the flux sensitivity to $1\,\mu\Phi_0/\sqrt{\text{Hz}}$ with the current SQUID geometry would bring the spin sensitivity to $2000\,\mu_B/\sqrt{\text{Hz}}$. The sensitivity can also be increased by placing the dipole in the corner of the pickup loop instead of at the center. As noted above, smaller pickup loops would improve this further; in order to maximize the spin sensitivity the pickup loop should be as small as possible.

V. POTENTIAL FOR MEASURING PERSISTENT CURRENTS IN NORMAL-METAL RINGS

One of the main motivations for building this instrument is to measure persistent currents in normal-metal rings, as predicted by Büttiker, Imry, and Landauer.[18] They predicted the currents to be periodic in the flux threading the ring with a period of h/e. The first measurement of these currents in individual metal rings was performed by Chandrasekhar *et al.*[1] They found currents of 30 nA in a gold ring with a diameter of 2.4 μm and 6 nA in a rectangular loop of similar size. These currents are much larger than predicted theoretically. However, a more recent measurement by Jariwala *et al.* on an array of 30 gold rings with a diameter of 2.56 μm indicated that the currents may be significantly smaller, around 0.35 nA.[19] In contrast with the early measurements on metal rings, measurements of persistent currents in rings fabricated in a GaAs/AlGaAs two-dimensional electron gas, which have been performed by Mailly *et al.*, are in agreement with the theoretical predictions for those samples.[20]

The general arguments for using a scanning microscope for susceptibility measurements given in Sec. I are valid for measurements of persistent currents as well. Getting statistics on the behavior of several nominally identical rings is essential for understanding how the properties of individual rings relate to the ensemble properties of an array of rings. Being able to fabricate rings on different types of substrates and with different methods allows for a much broader range of comparisons. The measurements by Chandrasekhar *et al.*[1] clearly demonstrate that it is necessary to make reliable background measurements since they found that their raw data contained a large, aperiodic background signal, which in some cases varied between cooldowns.

For measuring persistent currents in normal-metal rings, the significant figure of merit is the sensitivity to a current in a micron-scale ring. In particular, assuming a ring with a diameter of 2 μm and the pickup loop 2 μm above the sample (modeled as a square with a side of 8 μm), the mutual inductance is about 0.5pH. This corresponds to a flux through the pickup loop of $2.5\times10^{-7}\,\Phi_0/\text{nA}$. Thus with the current SQUID geometry and assuming a flux sensitivity of $1\,\mu\Phi_0/\sqrt{\text{Hz}}$ we can reach a ring current sensitivity of 4 nA/Hz.

The ring current sensitivity can be improved further by improving the pickup loop design, just as the spin sensitivity; however, for this measurement the pickup loop should preferably be matched to the sample, not necessarily as small as possible. Again using 2 μm rings as an example, at a height of 0.5 μm the coupling is maximized with a circular pickup loop around 3 μm in diameter, giving a mutual inductance of 1.2pH. The mutual inductance is changed by less than 1% as long as the ring is less than 100 nm off-center with respect to the pickup loop, making the measurement relatively insensitive to positioning errors and vibrations. Assuming a SQUID flux sensitivity of $1\,\mu\Phi_0/\sqrt{\text{Hz}}$, the ring current sensitivity would then be 1.7 nA/Hz. This would allow us to measure currents on the order of those reported by Chandrasekhar *et al.* with an averaging time of no more than a few seconds for each level of the applied background field. With longer,

but still feasible, measurement times, a total ring current sensitivity of 0.1 nA is possible.

The instrument is, in its current state, suitable for various studies of magnetic materials on a mesoscopic length scale. We have identified improvements in the system that would improve sensitivity and make measurements of persistent currents in normal-metal rings possible at the expected current levels.

ACKNOWLEDGMENTS

The authors thank M. Ketchen for the original SQUID design, M. Huber for assistance in SQUID characterization, E. Straver for fabrication of the Sn dot sample, and B. Cabrera and A. Miller for providing the W TES sample and performing the transport measurements on it. Funding was provided by a Terman fellowship and by NSF Grants No. DMR-9802719 and No. DMR-9875193.

[1] V. Chandrasekhar, R. A. Webb, M. J. Brady, M. B. Ketchen, W. J. Gallagher, and A. Kleinsasser, Phys. Rev. Lett. **67**, 3578 (1991).
[2] J. R. Kirtley and J. P. Wickswo, Jr., Annu. Rev. Mater. Sci. **29**, 117 (1999).
[3] K. Hasselbach, C. Veauvy, and D. Mailly, Physica C **332**, 140 (2000).
[4] M. B. Ketchen, D. D. Awschalom, W. J. Gallagher, A. W. Kleinsasser, R. L. Sandstrom, J. R. Rozen, and B. Bumble, IEEE Trans. Magn. **MAG-25**, 1212 (1989).
[5] M. B. Ketchen, T. Kopley, and H. Ling, Appl. Phys. Lett. **44**, 1008 (1984).
[6] M. A. McCord and D. D. Awschalom, Appl. Phys. Lett. **57**, 2153 (1990).
[7] L. R. Narasimhan, M. Takigawa, and M. B. Ketchen, Appl. Phys. Lett. **65**, 1305 (1994).
[8] D. D. Awschalom and J. Warnock, IEEE J. Quantum Electron. **25**, 2570 (1989).
[9] B. W. Gardner, J. C. Wynn, P. G. Björnsson, E. W. J. Straver, K. A. Moler, J. R. Kirtley, and M. B. Ketchen, Rev. Sci. Instrum. **72**, 2361 (2001).
[10] J. Siegel, J. Witt, N. Venturi, and S. Field, Rev. Sci. Instrum. **66**, 2520 (1995).
[11] Hypres design rules, http://www.hypres.com/designrule/rules.html (as of Jan. 15, 2001).
[12] J. R. Kirtley, M. B. Ketchen, K. G. Stawiasz, J. Z. Sun, W. J. Gallagher, S. H. Blanton, and S. J. Wind, Appl. Phys. Lett. **66**, 1138 (1995).
[13] A. M. Chang, H. D. Hallen, L. Harriott, H. F. Hess, H. L. Kao, J. Kwo, R. E. Miller, R. Wolfe, J. van der Ziel, and T. Y. Chang, Appl. Phys. Lett. **61**, 1974 (1992).
[14] B. Cabrera, R. M. Clarke, P. Colling, A. J. Miller, S. Nam, and R. W. Romani, Appl. Phys. Lett. **73**, 735 (1998).
[15] J. R. Kirtley, C. C. Tsuei, K. A. Moler, V. G. Kogan, J. R. Clem, and A. J. Tuberfield, Appl. Phys. Lett. **74**, 4011 (1999).
[16] Including the effects of the finite coherence length would tend to further spread out the vortices giving a lower value for the penetration depth. However, the coherence length is normally small on the scale of the SQUID, so the effect of the finite coherence length is likely to be small.
[17] M. B. Ketchen, M. Bushan, S. B. Kaplan, and W. J. Gallagher, IEEE Trans. Magn. **27**, 3005 (1991).
[18] M. Büttiker, Y. Imry, and R. Landauer, Phys. Lett. **96A**, 365 (1983).
[19] E. M. Q. Jariwala, P. Mohanty, M. B. Ketchen, and R. A. Webb, Phys. Rev. Lett. **86**, 1594 (2001).
[20] D. Mailly, C. Chapelier, and A. Benoit, Phys. Rev. Lett. **70**, 2020 (1993).